

# Limiting the effects of earthquakes on gravitational-wave interferometers

Matthew Robert Perry<sup>1</sup>, Paul S Earle<sup>2</sup>, Michelle R Guy<sup>1</sup>, Jan Harms<sup>3</sup>, Michael Coughlin<sup>4</sup>, Sebastien Biscans<sup>5</sup>, Christopher Buchanan<sup>6</sup>, Eric Coughlin<sup>7</sup>, Jeremy Fee<sup>8</sup> and Nikhil Mukund<sup>9</sup>

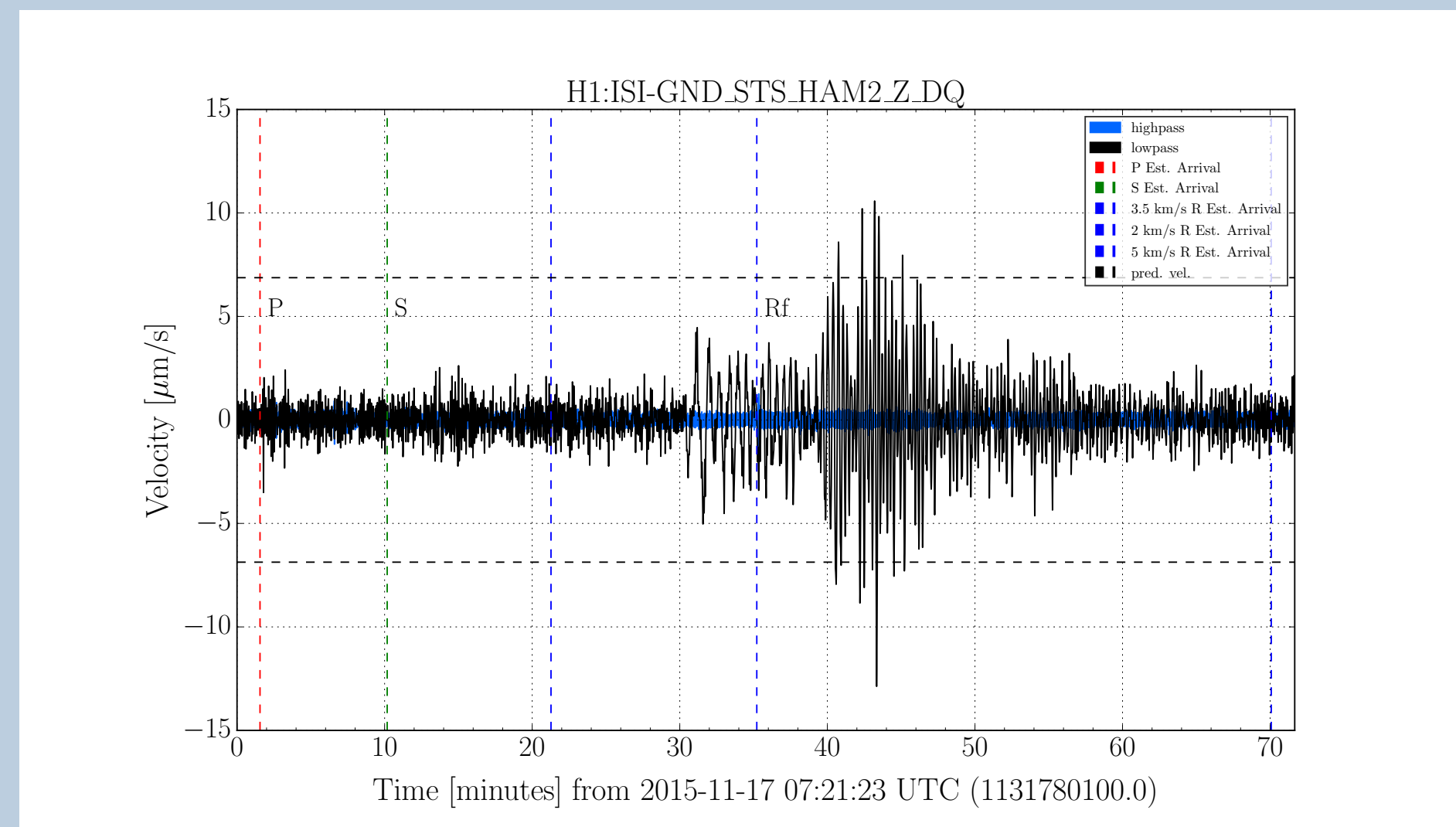
(1)USGS National Earthquake Information Center Golden, Golden, CO, United States, (2)USGS, Baltimore, MD, United States, (3)INFN, Firenze, Italy, (4)Harvard University, Physics, Cambridge, MA, United States, (5)Massachusetts Institute of Technology, Cambridge, MA, United States, (6)Louisiana State University, Department of Physics and Astronomy, Baton Rouge, LA, United States, (7)Luther College, Department of Computer Science, Decorah, IA, United States, (8)USGS Central Region Offices Denver, Denver, CO, United States, (9)University of Pune, Inter-University Centre for Astronomy and Astrophysics, Pune, India



## Introduction

- Second-generation ground-based gravitational wave interferometers such as the Laser Interferometer Gravitational-wave Observatory (LIGO) are susceptible to high-amplitude teleseismic events, which can cause astronomical detectors to fall out of mechanical lock (lockloss).
- Here we describe an early warning system for modern gravitational-wave observatories, which relies on near real-time earthquake alerts provided by the U.S. Geological Survey (USGS) and the National Oceanic and Atmospheric Administration (NOAA).
- Our initial results indicate that by using detector control configuration changes, we could save lockloss from 40-100 earthquakes events in a 6-month time-period.

## Notices



Ground motion from a seismometer at the LIGO Hanford site located in Washington, USA for the Nov 17, 2015 6.5 magnitude earthquake in Greece.

- Relies on the most preliminary notices of earthquakes currently available generated by worldwide networks of seismometers.
- USGS provides preliminary estimates of the location, including latitude, longitude, and depth, are provided.
- These solutions are distributed through USGS's Product Distribution Layer (PDL), which has been configured to receive all notifications of earthquakes worldwide.

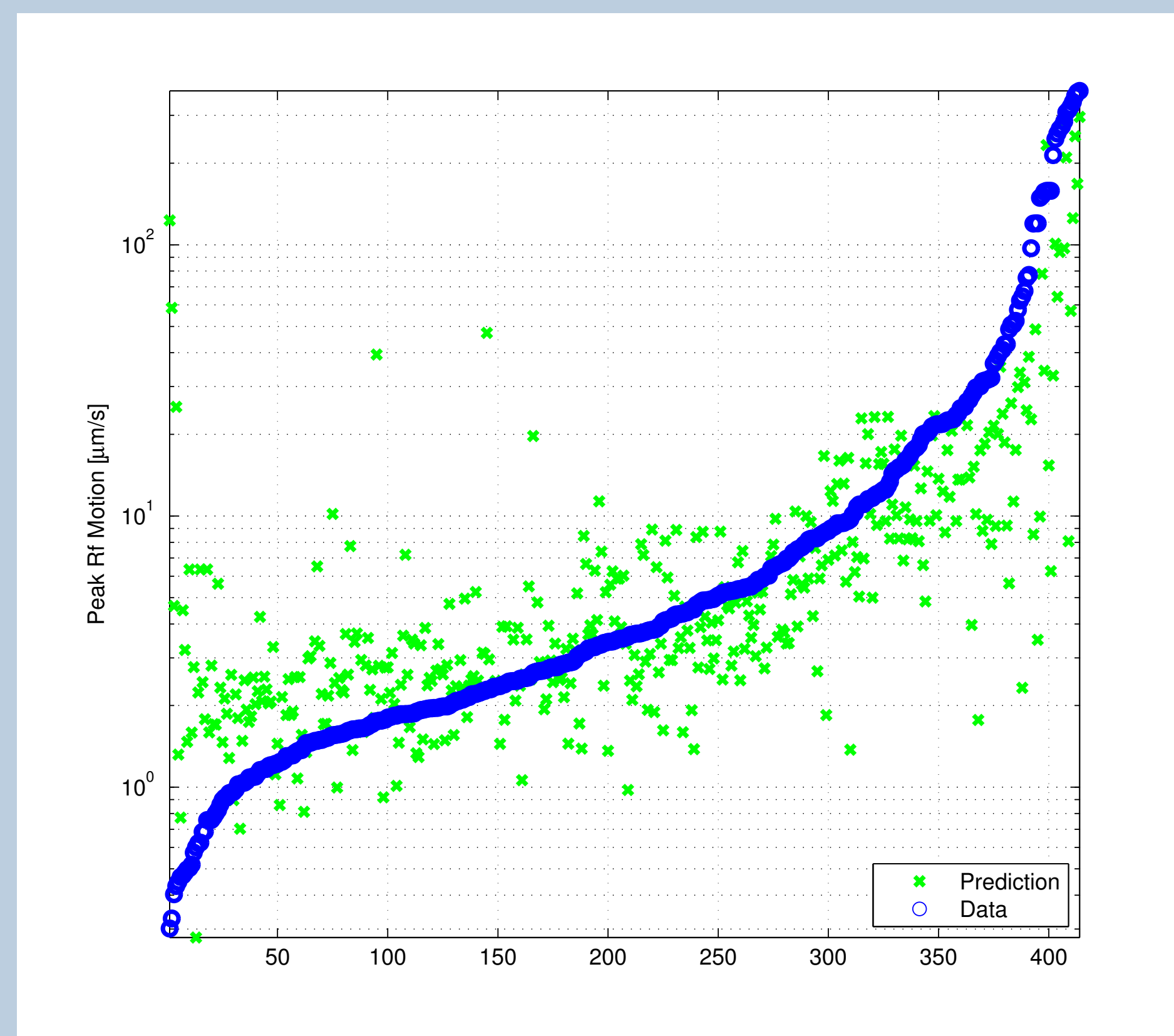
## Epics

- The final step of the process is to use the site amplitude and time-of-arrival predictions to create warnings (and possibly detector state changes) for the detectors.
- The algorithm analyzes the recent notifications and places a threshold on the predictions.
- We provide an epics variable that contains the following information: amplitude prediction, probability of lockloss, earthquake time-of-arrival

## Acknowledgements

MC was supported by the National Science Foundation Graduate Research Fellowship Program, under NSF grant number DGE 1144152.

## Ground Velocity Prediction

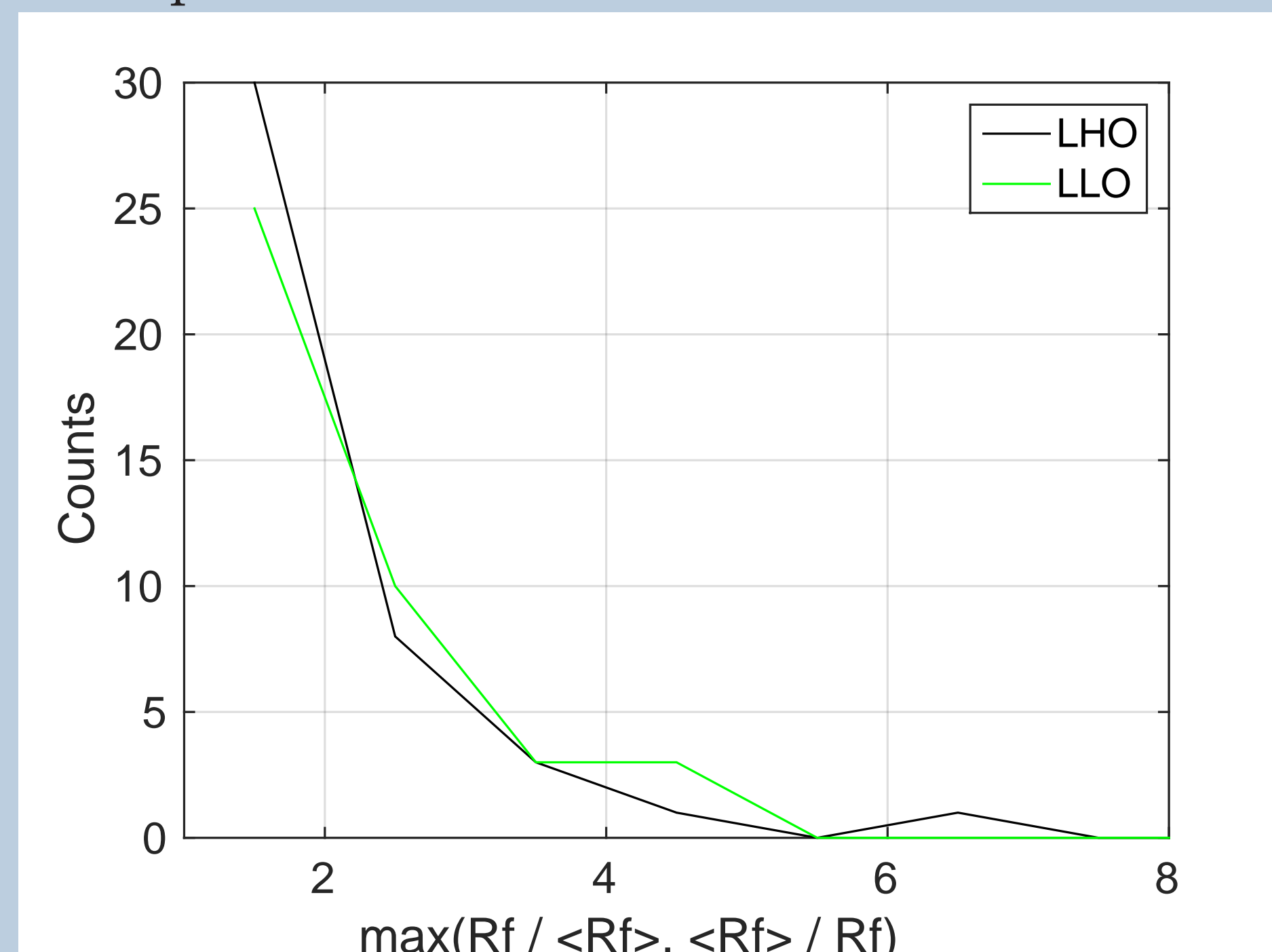


Fit of peak velocities seen during S5-S6 at the LHO interferometer to equation 1.

We estimate the peak amplitude of the surface waves,  $Rf_{amp}$ , at the sites using equation 1. We estimate the amplitude of the surface waves,  $Rf_{amp}$ , at the sites using the equation:

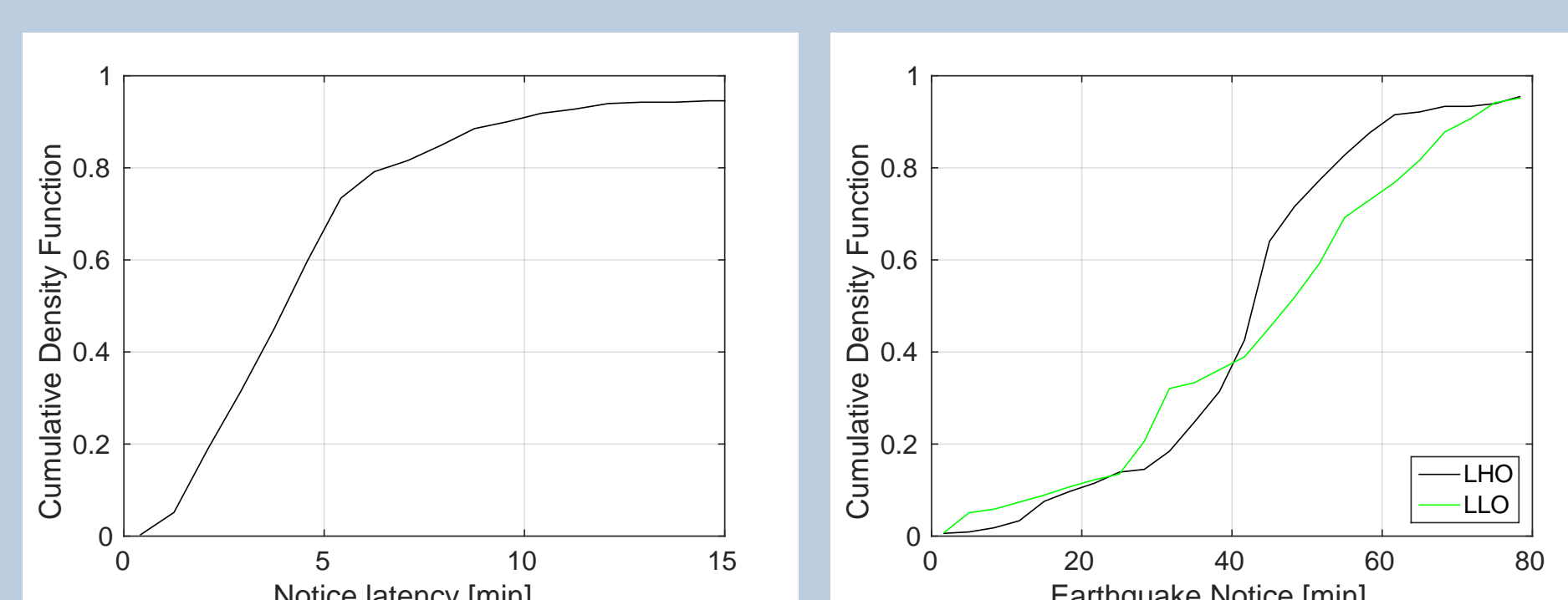
$$Rf_{amp} = 10^{-3} M A f e^{-2\pi h f_c / c d} / r^{rs} \quad (1)$$

where  $f_c = 10^{2.3-M/2}$ ,  $Af = \frac{Rf_0}{f_c R_{fs}}$ ,  $M$  is the magnitude of the earthquake,  $d$  is the distance,  $h$  is the depth of the earthquake,  $c$  is the speed of the surface-waves, and  $f_c$  is the corner frequency. These parameters are derived from minimizing the difference between the amplitude seen at the interferometer and that predicted by the equation.



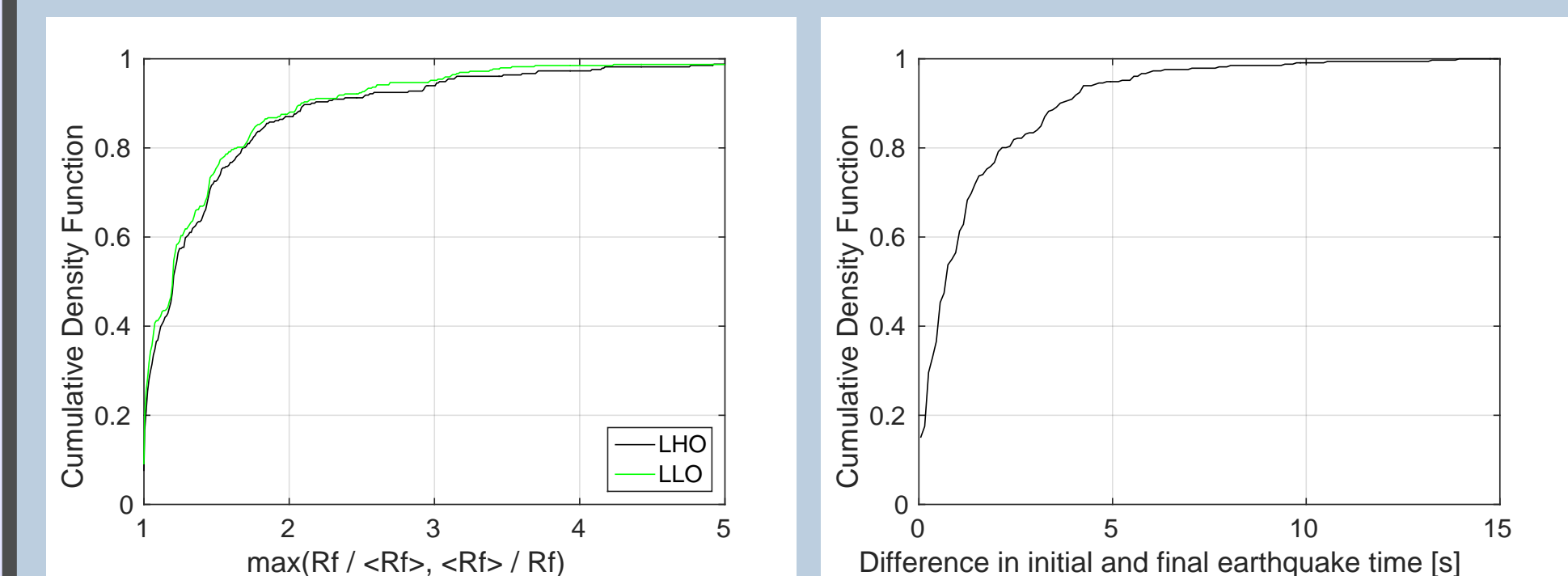
An important quality for an earthquake monitor is the accuracy of the ground-motion amplitude prediction and the time-of-arrival. We show the performance of estimation of peak velocities seen during O1 at the interferometers (LHO and LLO) using fit parameters estimated from S5-S6 data. About 94% of events are within a factor of 5, while those that are not are almost exclusively events that are due to the overlap of many events.

## Notification latency



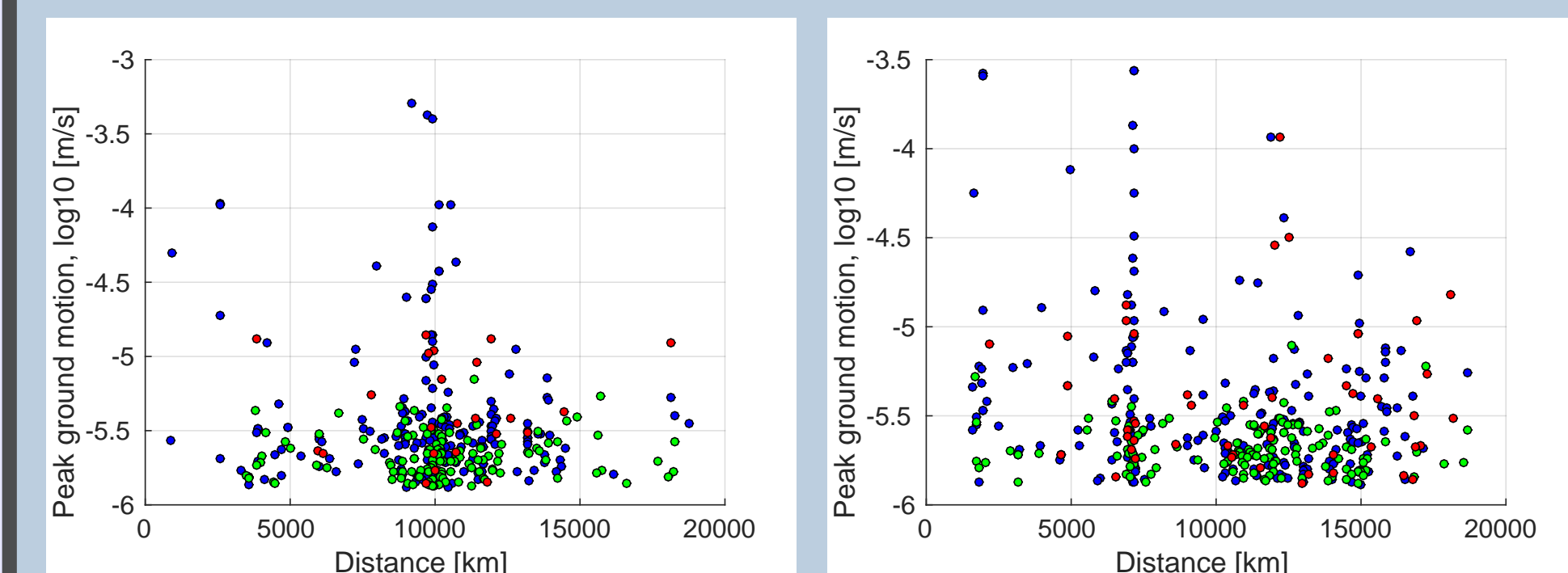
On the left, we show the time delay between the earthquake and generation of the PDL client notification. In general, notices are generated within 5 minutes of the earthquake. On the right, the cumulative probability distribution

## Effect of early notices

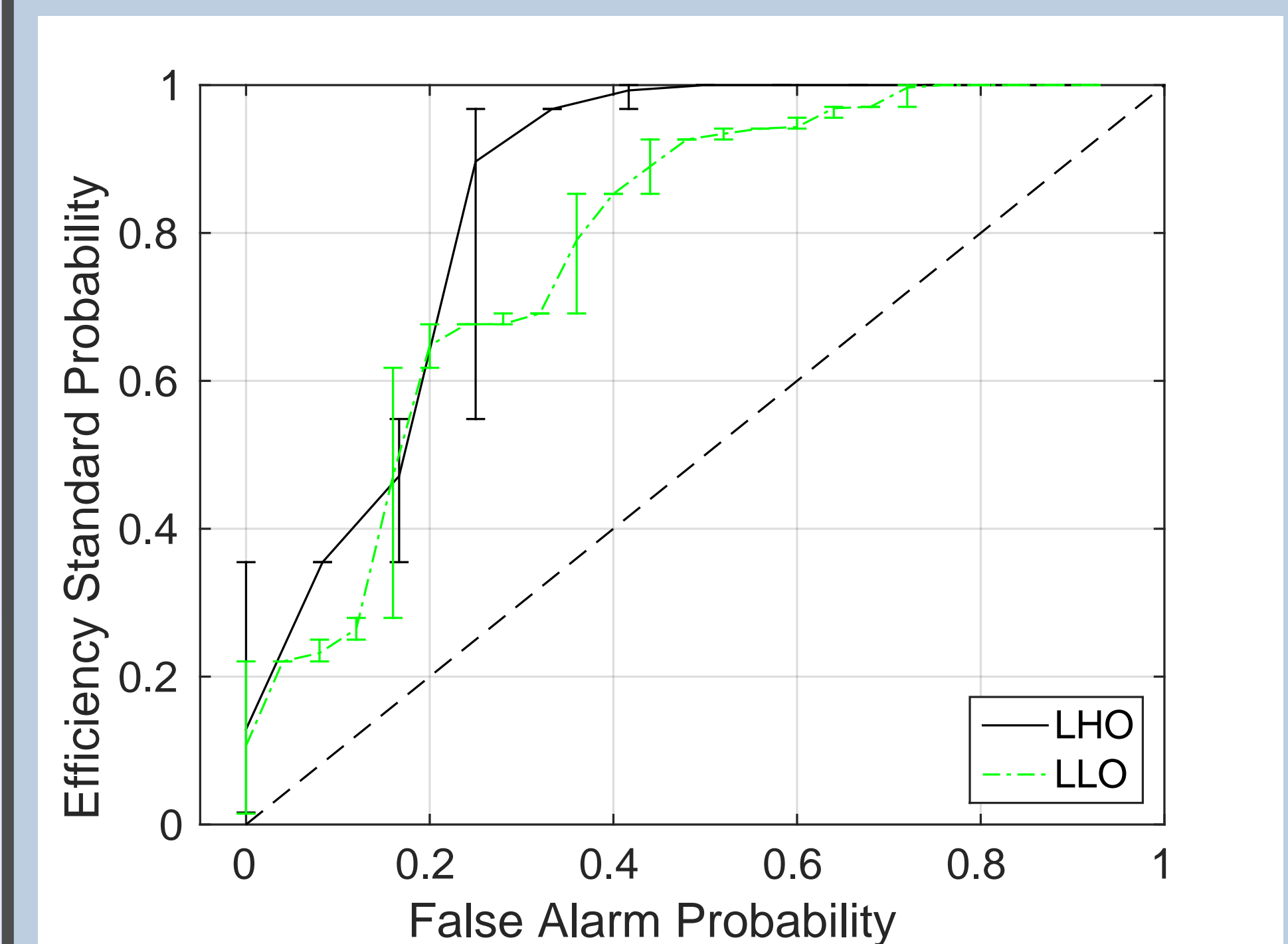


We use the earliest available notices for making time-of-arrival and amplitude predictions. Because the earliest notices may only rely on a few seismometers, as well as the fact that large earthquakes do not fault all at once, the estimates for both magnitude, depth, location, and time can be off. On the left is the difference of predicted peak velocities seen during O1 at the interferometers (LHO and LLO) using the initial and final estimates. About 90% of events are within a factor of 2 of the final predicted value. On the right is the difference between the initial and final estimates of the earthquake time. About 90% of early estimates are within 4 s of the final time.

## Lockloss prediction performance



We now measure the amplitude of the seismic ground motion that causes the detector to lose lock. We show these times, both for those times when lock losses occurred (red), when they did not (green), and when the detector was not locked (blue). In general, the plot shows that while in general ground velocities greater than about  $5 \mu\text{m/s}$  lead to lock loss, the situation is complicated at lower ground velocities.



We use a Machine Learning Algorithm to develop a lockloss prediction model. Above, we show the efficiency curves using the earthquake parameter derived parameters. The curves which include the observed ground velocity at the sites are similar. In general, there is a tradeoff between false alarm probability and efficiency standard probability. For example, if we adopt a false alarm probability threshold of 0.5, between 90-100% of earthquakes can be caught.